Influence of laser parameters and staining on femtosecond laser-based intracellular nanosurgery

K. Kuetemeyer,* R. Rezgui, H. Lubatschowski, and A. Heisterkamp

Laser Zentrum Hannover e.V., Hollerithallee 8, 30419 Hannover, Germany

*k.kuetemeyer@lzh.de

Abstract: Femtosecond (fs) laser-based intracellular nanosurgery has become an important tool in cell biology, albeit the mechanisms in the so-called low-density plasma regime are largely unknown. Previous calculations of free-electron densities for intracellular surgery used water as a model substance for biological media and neglected the presence of dye and biomolecules. In addition, it is still unclear on which time scales free-electron and free-radical induced chemical effects take place in a cellular environment. Here, we present our experimental study on the influence of laser parameters and staining on the intracellular ablation threshold in the low-density plasma regime. We found that the ablation effect of fs laser pulse trains resulted from the accumulation of single-shot multiphoton-induced photochemical effects finished within a few nanoseconds. At the threshold, the number of applied pulses was inversely proportional to a higher order of the irradiance, depending on the laser repetition rate and wavelength. Furthermore, fluorescence staining of subcellular structures before surgery significantly decreased the ablation threshold. Based on our findings, we propose that dye molecules are the major source for providing seed electrons for the ionization cascade. Consequently, future calculations of free-electron densities for intracellular nanosurgery have to take them into account, especially in the calculations of multiphoton ionization rates.

OCIS codes: (170.0170) Medical optics and biotechnology; (180.4315) Nonlinear microscopy; (190.4180) Multiphoton processes.

References and links

1. K. Koenig, I. Riemann, P. Fischer, and K. H. Halbhuber, "Intracellular nanosurgery with near infrared femtosecond laser pulses," Cell Mol. Biol. **45,** 195–201 (1999).
2. K. Koenig, I. Riemann, and W. Fritzsche, "Nanodissection of human chromosomes with near-infrared femtosecond laser pulses," Opt. Lett. **26,** 819–821 (2001).
3. U. K. Tirlapur and K. Koenig, "Targeted transfection by femtosecond laser," Nature **418,** 290–291 (2002).
4. W. Watanabe, N. Arakawa, T. Higashi, K. Fukui, K. Isobe, K. Itoh, and S. Matsunaga, "Femtosecond laser disruption of subcellular organelles in a living cell," Opt. Express **12,** 4203–4213 (2004).
5. I. Maxwell, S. Chung, and E. Mazur, "Nanoprocessing of subcellular targets using femtosecond laser pulses," Med. Laser Appl. **20,** 193–200 (2005).
6. M. F. Yanik, H. Cinar, H. N. Cinar, A. D. Chisholm, Y. Jin, and A. Ben-Yakar, "Functional regeneration after laser axotomy," Nature **432,** 822–822 (2004).
7. W. Supatto, D. Debarre, B. Moulia, E. Brouzes, J. L. Martin, E. Farge, and E. Beaurepaire, "In vivo modulation of morphogenetic movements in Drosophila embryos with femtosecond laser pulses," Proc. Natl. Acad. Sci. USA **102,** 1047–1052 (2005).

#132149 - $15.00 USD Received 22 Jul 2010; revised 5 Aug 2010; accepted 5 Aug 2010; published 10 Aug 2010

8. L. Sacconi, R. P. O'Connor, A. Jasaitis, A. Masi, M. Buffelli, and F. S. Pavone, "In vivo multiphoton nanosurgery on cortical neurons," J. Biomed. Opt. **12,** 050502 (2007).
9. A. L. Allegra Mascaro, L. Sacconi, and F. S. Pavone, "Multi-photon nanosurgery in live brain," Front. Neuroenerg. **2,** 21 (2010).
10. A. Vogel, J. Noack, G. Huettman, and G. Paltauf, "Mechanisms of femtosecond laser nanosurgery of cells and tissues," Appl. Phys. B **81,** 1015–1047 (2005).
11. A. Heisterkamp, I. Z.Maxwell, J. M. Underwood, J. A. Nickerson, S. Kumar, D. E. Ingber, and E. Mazur, "Pulse energy dependence of subcellular dissection by femtosecond laser pulses," Opt. Express **13,** 3690–3696 (2005).
12. L. Sacconi, I. M. Tolic-Norrelykke, R. Antolini, and F. S. Pavone, "Combined intracellular three-dimensional imaging and selective nanosurgery by a nonlinear microscope," J. Biomed. Opt. **10,** 014002 (2005).
13. S. Kumar, I. Z. Maxwell, A. Heisterkamp, T. R. Polte, T. P. Lele, M. Salanga, E. Mazur, and D. E. Ingber, "Viscoelastic retraction of single living stress fibers and its impact on cell shape, cytoskeletal organization, and extracellular matrix mechanics," Biophys. J. **90,** 3762–3773 (2006).
14. T. Shimada, W. Watanabe, S. Matsunaga, T. Higashi, H. Ishii, K. Fukui, K. Isobe, and K. Itoh, "Intracellular disruption of mitochondria in a living HeLa cell with a 76-MHz femtosecond laser oscillator," Opt. Express **13,** 9869–9880 (2005).
15. K. Kuetemeyer, A. Lucas-Hahn, B. Petersen, E. Lemme, P. Hassel, H. Niemann, and A. Heisterkamp, "Combined multiphoton imaging and automated functional enucleation of porcine oocytes using femtosecond laser pulses," J. Biomed. Opt. **15,** 046006 (2010).
16. F. Bourgeois and A. Ben-Yakar, "Femtosecond laser nanoaxotomy properties and their effect on axonal recovery in C.elegans," Opt. Express **15,** 8521–8531 (2007).
17. P. K. Kennedy, S. A. Boppart, D. X. Hammer, B. A. Rockwell, G. D. Noojin, and W.P. Roach, "A first-order model for computation of laser-induced breakdown thresholds in ocular and aqueous-media: part II - comparison to experiment," IEEE J. Quantum Electron. **31,** 2250–2257 (1995).
18. A. Vogel, N. Linz, S. Freidank, and G. Paltauf, "Femtosecond-laser-induced nanocavitation in water: Implications for optical breakdown threshold and cell surgery," Phys. Rev. Lett. **100,** 038102 (2008).
19. B. Boudaiffa, P. Cloutier, D. Hunting, M. A. Huels, and L. Sanche, "Resonant formation of DNA strand breaks by low-energy (3 to 20 eV) electrons," Science **287,** 1658–1660 (2000).
20. L. Sanche, "Low energy electron-driven damage in biomolecules," Eur. Phys. J. D **35,** 367–390 (2005).
21. D. N. Nikogosyan, A. A. Oraevsky, and V. I. Rupasov, "Two-photon ionization and dissociation of liquid water by powerful laser UV radiation," Chem. Phys. **77,** 131–143 (1983).
22. F. Hutchinson, "Chemical-changes induced in DNA by ionizing-radiation," Prog. Nucleic Acid Res. Mol. Biol. **32,** 115–154 (1985).
23. A. A. Oraevsky and D. N. Nikogosyan, "Picosecond two-quantum UV photochemistry of thymine in aqueous-solution," Chem. Phys. **100,** 429–445 (1985).
24. U. K. Tirlapur, K. Koenig, C. Peuckert, R. Krieg, and K. J. Halbhuber, "Femtosecond near-infrared laser pulses elicit generation of reactive oxygen species in mammalian cells leading to apoptosis-like death," Exp. Cell Res. **263,** 88–97 (2001).
25. J. Baumgart, K. Kuetemeyer, W. Bintig, A. Ngezahayo, W. Ertmer, H. Lubatschowski, and A. Heisterkamp, "Repetition rate dependency of reactive oxygen species formation during femtosecond laser-based cell surgery," J. Biomed. Opt. **14,** 054040 (2009).
26. K. Kuetemeyer, J. Baumgart, H. Lubatschowski, and A. Heisterkamp, "Repetition rate dependency of low-density plasma effects during femtosecond-laser-based surgery of biological tissue," Appl. Phys. B **97,** 695–699 (2009).
27. F. Bestvater, E. Spiess, G. Stobrawa, M. Hacker, T. Feurer, T. Porwol, U. Berchner-Pfannschmidt, C. Wotzlaw, and H. Acker, "Two-photon fluorescence absorption and emission spectra of dyes relevant for cell imaging," J. Microsc-Oxford **208,** 108–115 (2002).
28. F. Helmchen and W. Denk, "Deep tissue two-photon microscopy," Nat. Met. **2,** 932–940 (2005).
29. J. L. Boulnois, "Photophysical processes in recent medical laser developments: a review," Laser Med. Sci. **1,** 47–66 (1986).
30. A. P. Reuvers, C. L. Greenstock, J. Borsa, and J. D. Chapman, "Studies on mechanism of chemical radioprotection by dimethyl sulfoxide," Int. J. Radiat. Biol. **24,** 533–536 (1973).
31. R. Roots and S. Okada, "Estimation of life times and diffusion distances of radicals involved in X-ray-induced DNA strand breaks or killing of mammalian cells," Radiat. Res. **64,** 306–320 (1975).
32. J. F. Ward, "DNA damage produced by ionizing radiation in mammalian cells: identities, mechanisms of formation, and reparability," Prog. Nucleic Acid Res. Mol. Biol. **35,** 95–125 (1988).
33. E. S. Williams, J. Stap, J. Essers, B. Ponnaiya, M. S. Luijsterburg, P. M. Krawczyk, R. L. Ullrich, J. A. Aten, and S. M. Bailey, "DNA double-strand breaks are not sufficient to initiate recruitment of TRF2," Nat. Genet. **39,** 696–698 (2007).
34. C. Dinant, M. de Jager, J. Essers, W. A. van Cappellen, R. Kanaar, A. B. Houtsmuller, and W. Vermeulen, "Activation of multiple DNA repair pathways by subnuclear damage induction methods," J. Cell Sci. **120,** 2731–2740 (2007).
35. J. E. Downing, W. M. Christopherson, and W. L. Broghamer, "Nuclear water content during carcinogenesis,"

#132149 - $15.00 USD Received 22 Jul 2010; revised 5 Aug 2010; accepted 5 Aug 2010; published 10 Aug 2010

Cancer **15,** 1176–1180 (1962).
36. H. M. Golomb and G. F. Bahr, "Electron-microscopy of human interphase nuclei - determination of total dry mass and DNA-packing ratio," Chromosoma **46,** 233–245 (1974).
37. F. G. Loontiens, P. Regenfuss, A. Zechel, L. Dumortier, and R. M. Clegg, "Binding characteristics of Hoechst 33258 with calf thymus DNA, Poly[d(A-T)], and d(CCGGAATTCCGG): multiple stoichiometries and determination of tight binding with a wide spectrum of site affinities," Biochemistry-US **29,** 9029–9039 (1990).
38. I. Cohanoschi and F. E. Hernandez, "Surface plasmon enhancement of two- and three-photon absorption of Hoechst 33 258 dye in activated gold colloid solution," J. Phys. Chem. B **109,** 14506–14512 (2005).
39. A. Rosenfeld, M. Lorenz, R. Stoian, and D. Ashkenasi, "Ultrashort-laser-pulse damage threshold of transparent materials and the role of incubation," Appl. Phys. A **69,** S373–S376 (1999).
40. Y. Jee, M. F. Becker, and R. M. Walser, "Laser-induced damage on single-crystal metal surfaces," J. Opt. Soc. Am. B **5,** 648–659 (1988).
41. F. Williams, S. P. Varma, and S. Hillenius, "Liquid water as a lone-pair amorphous-semiconductor," J. Chem. Phys. **64,** 1549–1554 (1976).
42. H. Goerner, "Direct and sensitized photoprocesses of bis-benzimidazole dyes and the effects of surfactants and DNA," Photochem. Photobiol. **73,** 339–348 (2001).
43. E. Amouyal, A. Bernas, and D. Grand, "On the photoionization energy threshold of tryptophan in aqueous solutions," Photochem. Photobiol. **29,** 1071–1077 (1979).

1. Introduction

Since its first demonstration by Koenig et al. in 1999 [1], femtosecond (fs) laser cell surgery has proven to be an excellent tool for minimally invasive and extremely precise manipulation of single cells, both in-vitro [2–5] and in-vivo [6–9]. When fs laser pulses are focused by high numerical aperture objectives (NA $\geq$ 0.8) into biological media, the created photon densities are sufficient to induce multiphoton ionization in a sub-femtoliter volume. Together with cascade ionization, very high free-electron densities are generated, resulting in plasma-mediated ablation of biological material with cut sizes below 100 nm [2, 10].

Intracellular nanosurgery with fs laser pulses has become an important tool in cell biology. Cutting single cytoskeletal fibers without affecting adjacent structures allows for local perturbation of the cytoskeleton [11, 12]. This process helps to understand the organization and function of this key cellular structure and provides insight into cell motility, differentiation, and apoptosis [13]. Selective disruption of individual mitochondria can be used to study their role in energy production, cell death and subcellular homeostasis [4, 14]. Recently, automated ablation of entire metaphase plates in porcine oocytes has been published by our group [15]. This method may serve as an alternative for conventional highly-invasive enucleation techniques of somatic cell cloning. As the contrast between subcellular structures is usually very weak in all of these applications, the organelle of interest has to be stained with fluorescent dyes or tagged with fluorescent proteins. Therefore, intracellular nanosurgery is often combined with fluorescence [11], confocal laser scanning [4, 13, 14] or multiphoton microscopy [12, 15].

Two parameter regimes have been established for fs laser cell surgery. One approach employs one to several hundred amplified pulses with repetition rates around 1 kHz and pulse energies of a few to tens of nanojoule [4, 11, 16]. In this regime, the generated free-electron densities are likely sufficient to induce cavitation bubble and shock wave formation. The abrupt expansion of the cavitation bubble causes photodisruption in biological media [17, 18]. The other approach uses long pulse trains (several thousand to million pulses) from laser oscillators with repetition rates around 80 MHz and pulse energies well below the optical breakdown threshold [2, 12, 14]. A so-called low-density plasma is produced in this regime which leads to free-electron induced chemical decomposition (bond breaking) of biomolecules [10, 19, 20]. In addition, reactive oxygen species (ROS) are yielded by multiphoton ionization and dissociation of water molecules, such as the hydroxyl radical ($OH^{\bullet}$) or superoxide (O_2^-) [21]. ROS are known to react efficiently with biomolecules, such as DNA bases, and may induce cell death at high concentrations [22-24]. The accumulation of the described chemical effects over many pulses

#132149 - $15.00 USD Received 22 Jul 2010; revised 5 Aug 2010; accepted 5 Aug 2010; published 10 Aug 2010

leads to ablation of biological material.

Although extensive theoretical work has been done by Vogel et al. to understand the fundamental mechanisms in the low-density plasma regime, their calculations of free-electron densities used water as a model substance for biological media [10]. The influence of dye and biomolecules on the multiphoton and cascade ionization rates was neglected. However, Koenig et al. showed that labeling single chromosomes with Giemsa reduced the ablation threshold by a factor of 2.7 [2]. Furthermore, it is still unclear on which time scales free-radical and free-electron induced chemical effects take place in a cellular environment. Nikogosyan et al. showed that photochemical processes leading to generation of ROS in aqueous solution can be classified into fast and slow reactions with time constants in the nano- to microsecond and millisecond range, respectively [21]. Recent experimental studies by our group revealed an influence of the laser repetition rate on the efficiency of ROS formation in cells and tissue [25, 26]. Consequently, the time interval between two successive laser pulses may affect the ablation threshold of subcellular structures.

In this paper, we investigated the influence of laser parameters and staining on the ablation threshold of subcellular structures in the low-density plasma regime. Hoechst-stained cell nuclei, used as a model substance for intracellular surgery, were irradiated in arbitrarily selected areas while the extent of apparent photodamage was evaluated using two-photon microscopy.

2. Materials and methods

2.1. Laser system and microscope

The laser system used in this study was a tunable Ti:sapphire laser (Chameleon Ultra II, Coherent) which generates ultrashort pulses of 140 fs at a repetition rate of 80 MHz with a $M^2 < 1.1$ beam quality. The accessible wavelength ranges from 680 to 1080 nm and the maximum pulse energy at 800 nm is 44 nJ at the laser output. An acousto optical pulse picker (Pulse Select, APE GmbH) was applied to regulate the pulse frequency for the manipulation of single cells by selecting pulses of the laser beam with a division ratio between 1:20 and 1:80000 (corresponding to 4 MHz and 1 kHz). These pulses are diffracted into the first order with a diffraction angle of approximately 3.5°. The diffracted and initial laser beam were used for cell manipulation and multiphoton microscopy, respectively (see manipulation and imaging beam in Fig. 1).

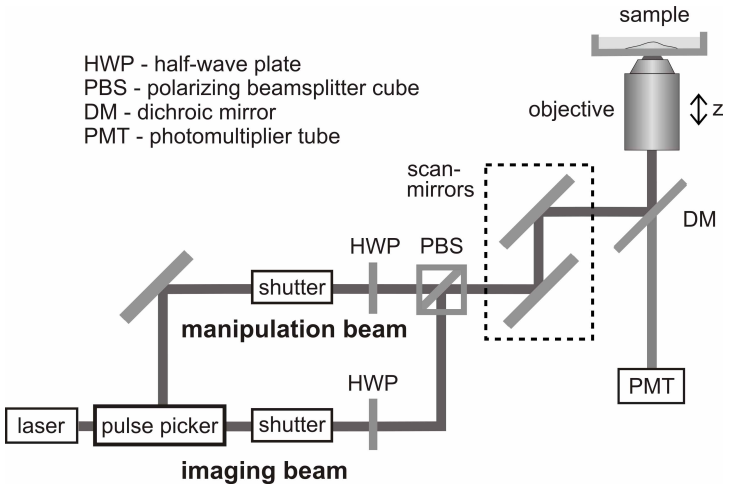

Fig. 1. Schematic setup for multiphoton imaging and manipulation of single cells.

#132149 - $15.00 USD Received 22 Jul 2010; revised 5 Aug 2010; accepted 5 Aug 2010; published 10 Aug 2010

Both laser beams were guided through a mechanical shutter and an attenuator, consisting of a half-wave plate and a polarizing beamsplitter cube, before being superimposed. After entering the tubus of an inverted microscope (Axiovert 100, Carl Zeiss AG) via a dichroic mirror, they were focused into the sample by a 1.3-NA oil immersion objective (Plan-Neofluar, Carl Zeiss AG). At a central wavelength of 720 nm, this results in a theoretical diffraction-limited spot diameter of approximately 1080 nm. Because of dispersion in the optics, the pulse duration in the sample was between 230 and 280 fs over the wavelength range determined with the autocorrelator "CARPE" (APE GmbH). Laser beam scanning in the x-y plane was achieved by a pair of high-speed galvanometer mirrors (Cambridge Technology). A piezoelectric objective-lens positioning system (nanoMIPOS 400, Piezosystem Jena GmbH) was used to move the laser focus along the z-axis. The fluorescence induced by multiphoton excitation at low pulse energies around 0.05 nJ passed the objective and the dichroic mirror in the backward direction and was detected by a photomultiplier tube (R6357, Hamamatsu Photonics).

2.2. Cell labeling and manipulation

Bovine endothelial cells were cultivated in glass bottom dishes with a thickness of 170 μm (MatTek Corporation) using RPMI 1640 medium (Roswell Park Memorial Institute) supplemented with 10% FCS (fetal calf serum) and the antibiotics penicillin, streptomycin, and partricin at 37^{o}C and 5% CO_2 humidified atmosphere. The dyes used in our experiments were the nucleic acid stains Hoechst 33342 (Invitrogen; final concentration: 5 μg/ml) and SYBR Green I (Invitrogen; final concentration: 1:1000 of the original 10,000x stock solution) and the membrane stain FM4-64 (Invitrogen; final concentration: 6 μg/ml).

For the live cell experiments, nuclear DNA was stained with Hoechst 33342 for 10 minutes at 37^{o}C. Prior to imaging and manipulation, cells were transferred into RPMI medium. The glass bottom dishes were placed into a microscope stage incubation system (Okolab), which was set to 37^{o}C and 5% CO_2 humidified atmosphere.

For the fixed cell experiments, cells were fixed in 4 % paraformaldehyde (Sigma Aldrich) in phosphate buffered saline (PBS) for 20 minutes and stained with either FM4-64 or both Hoechst 33342 and FM4-64 for 10 minutes. After imaging and manipulation in PBS medium at room temperature, cells were re-stained with Hoechst 33342.

Two-photon excitation of Hoechst 33342 and FM4-64 was done at a central wavelength of 720 and 800 nm, respectively, which corresponds to the two-photon absorption maximum of the Hoechst 33342 dye in this range [27]. For cell manipulation, the laser beam was either focused on a single point or scanned along a line in an arbitrarily selected area of the nucleus. Multiphoton microscopy images of each cell before and after manipulation were compared to evaluate the extent of apparent photodamage. Re-staining of the cells with Hoechst 33342 and SYBR Green I was done to discriminate photobleaching and ablation. The FWHM-width of the damaged region was measured by averaging over three positions along the laser cut.

3. Results

Varying the laser pulse energy for line cutting in stained cell nuclei at a fixed wavelength, repetition rate and spatial pulse overlap exhibited three distinct regimes. Above the first threshold, a clear dip in fluorescence could be observed a few minutes after irradiation [see Fig. 2(a)]. Above the second threshold, which was approximately 50% higher, the dip in fluorescence appeared directly after irradiation [see Fig. 2(b)]. Re-staining experiments with different nucleid acid stains resulted in a fluorescence recovery of the damaged region in the first, but not in the second case. Therefore, they are most likely corresponding to the photobleaching and ablation thresholds, which were first demonstrated and studied by Heisterkamp et al. [11]. Manipulation of more than 20 cells per pulse energy revealed that the ablation threshold varied about 30 per-

#132149 - $15.00 USD Received 22 Jul 2010; revised 5 Aug 2010; accepted 5 Aug 2010; published 10 Aug 2010

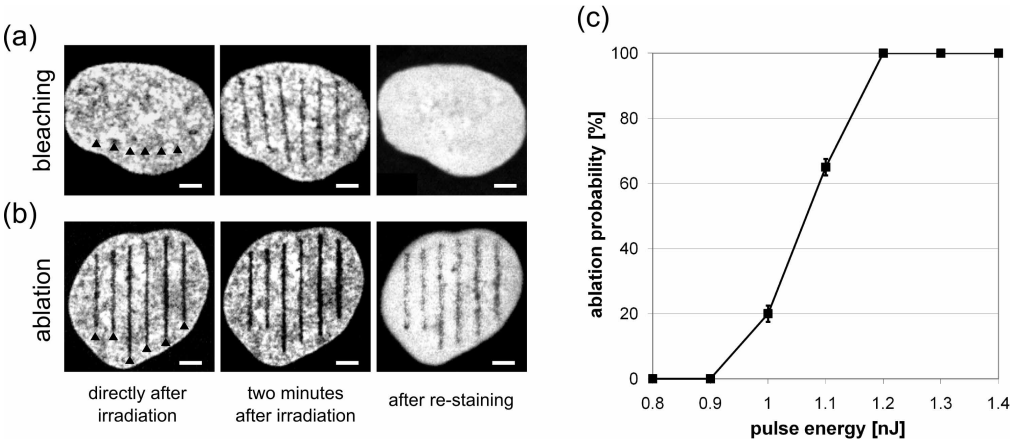

Fig. 2. (a,b) Multiphoton microscopy images of live Hoechst stained cell nuclei directly after and two minutes after line cutting (indicated by black triangles) and after re-staining. At pulse energies in the photobleaching regime, a clear dip in fluorescence could be observed after a few minutes. Above the ablation threshold, the dip in fluorescence occurred directly after irradiation. Scale bar: 3 μm. (c) Ablation probability as a function of the pulse energy at a fixed repetition rate of 40 kHz, a central wavelength of 720 nm and 200 pulses per micrometer (n $\geq$ 20 for each data point).

cent from cell to cell [see Fig. 2(c)]. Consequently, an ablation probability of 100 % in at least ten cell nuclei was defined as the overall ablation threshold in all further experiments.

To evaluate the influence of the time interval between two successive laser pulses on the ablation threshold, we varied the repetition rate between 1 kHz and 80 MHz at a central wavelength of 720 nm. The radiant energy density, defined as the number of laser pulses per micrometer, was kept constant by simultaneously adjusting the scanning speed of the line cuts. No significant influence of the laser repetition rate on the ablation threshold was observed for each constant radiant energy density [see Fig. 3(a)]. However, the threshold pulse energy increased from 0.25 nJ at 40,000 pulses per micrometer to 1.3 nJ at 100 pulses per micrometer. Changing the line scanning speed at a fixed repetition rate showed that the exposure time per micrometer was inversely proportional to approximately the fourth power of irradiance [see solid line in Fig. 3(b)]. With 5 mM ascorbic acid as an additional antioxidant in the culture medium, the same threshold pulse energies were measured (data not shown).

The influence of Hoechst molecules on the ablation process was studied by comparing the threshold pulse energies with and without previous Hoechst staining at a central wavelength of 720 nm. In this experiment, the time interval between manipulation and evaluation of the ablation was about 15 minutes due to cell re-staining. Because line cuts often disappeared in live cells over this time period as a result of chromatin movement, fixed cells were used instead. Concerning the ablation threshold, no difference was measured between live and fixed cell nuclei (data not shown). Membrane staining was done to identify the cell nucleus without Hoechst staining. At 1 MHz repetition rate and 20,000 pulses per micrometer each with 1.5 nJ, a clear dip in fluorescence was observed with Hoechst staining while no ablation occurred without it [see Fig. 4(a) and 4(b)]. In a logarithmic plot of the ablation probability vs. the pulse energy, the same slope was observed in both cases [see Fig. 4(c)]. However, the threshold pulse energy was a factor four lower with Hoechst staining. In agreement with Fig. 3, no influence of the repetition rate was observed without Hoechst staining [see slopes of 50 kHz and 1 MHz in Fig. 4(c)].

#132149 - $15.00 USD Received 22 Jul 2010; revised 5 Aug 2010; accepted 5 Aug 2010; published 10 Aug 2010

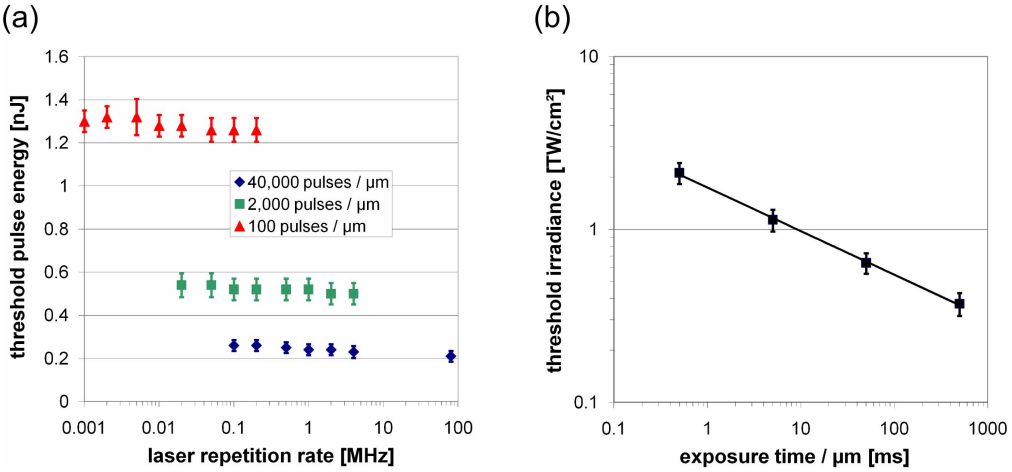

Fig. 3. (a) Ablation threshold pulse energy for line cuts in live Hoechst stained cell nuclei as a function of the repetition rate at different numbers of pulses per micrometer. No significant influence of the repetition rate was observed. (b) Ablation threshold irradiance as a function of the exposure time per micrometer at a fixed repetition rate of 40 kHz. The exposure time was inversely proportional to approximately the fourth power of irradiance (solid line). A central wavelength of 720 nm was used in all cases. Each data point represents the mean ± standard deviation of at least five experiments.

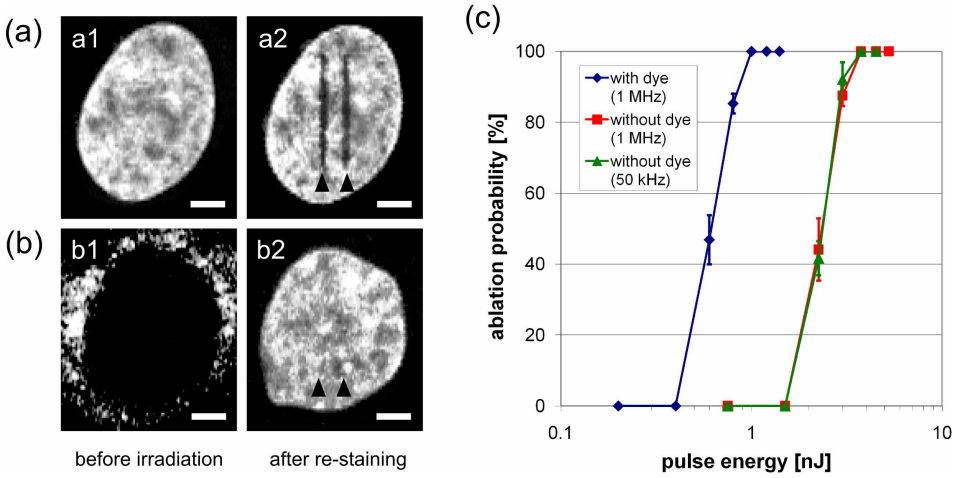

Fig. 4. Influence of Hoechst staining on the ablation threshold for line cuts in fixed cell nuclei. A central wavelength of 720 nm and 20,000 pulses per micrometer were used. Multiphoton microscopy images of (a) Hoechst / FM4-64 stained and (b) FM4-64 stained cell nuclei (a1;b1) before and (a2;b2) after line cutting at 1.5 nJ pulse energy (indicated by black triangles) and Hoechst re-staining. Scale bar: 3 μm. (c) Ablation probability as a function of the logarithmic pulse energy with and without Hoechst staining before line cutting. The ablation threshold was a factor four lower with Hoechst staining (n=3 experiments for each data point, the values represent the means ± standard deviation).

#132149 - $15.00 USD Received 22 Jul 2010; revised 5 Aug 2010; accepted 5 Aug 2010; published 10 Aug 2010

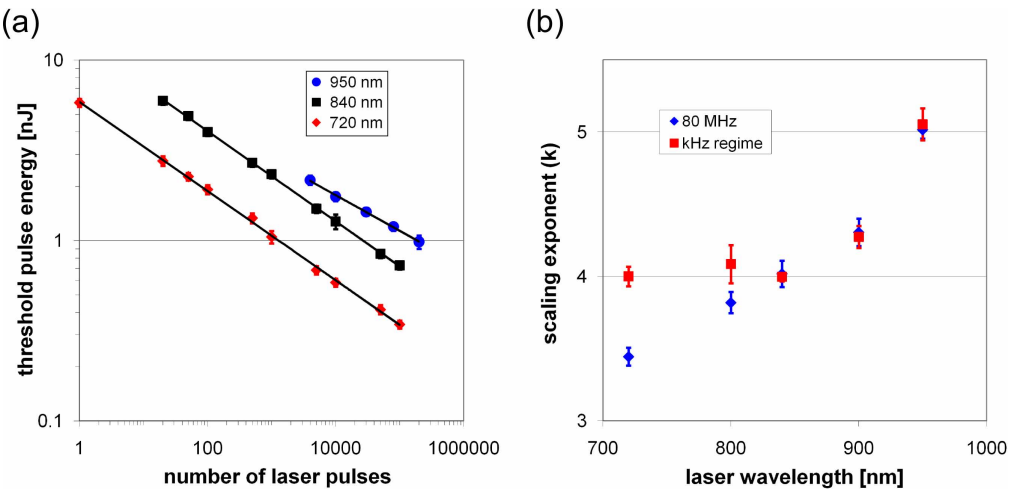

Fig. 5. (a) Wavelength dependence of the ablation threshold pulse energy as a function of the number of applied pulses on a single spot in live Hoechst stained cell nuclei at repetition rates in the kHz regime. Solid lines show the power-law fits for each wavelength. Between 840 and 950 nm, the scaling exponent increased from k=4 to k=5. (b) Scaling exponent k as a function of the laser wavelength at different repetition rates in the kHz regime and 80 MHz. Each data point represents the mean ± standard deviation of at least three experiments.

We studied the dependence of the ablation threshold on the number of applied laser pulses on a single spot (single point illumination). At a fixed repetition rate in the kHz regime, different wavelengths were used, from which three are exemplarily shown in Fig. 5(a). For each pulse train, the threshold pulse energy increased with the wavelength. Compared to 720 nm, about two-times and three-times higher pulse energies were required at 840 and 950 nm, respectively [see Fig. 5(a)]. Power-law fitting of the threshold data showed that the number of applied pulses was inversely proportional to the fourth power of irradiance (scaling exponent k=4) at 720 and 840 nm and the fifth power of irradiance (k=5) at 950 nm. To determine the influence of the repetition rate on this relationship, the same experiments were done at 80 MHz. The scaling exponent was significantly lower at 720 nm (k=3.5) and 800 nm (k=3.8), whereas no deviation was observed above 800 nm [see Fig. 5(b)].

The final set of experiments was done to determine the FWHM-width of the damaged region above the ablation threshold. At a central wavelength of 720 nm, different repetition rates between 20 kHz and 80 MHz were used. As expected, the width of the damaged region increased with the laser pulse energy for all repetition rates (see Fig. 6). Within the error bars, the same slope was observed for all repetition rates up to 4 MHz. At 2,000 pulses per micrometer, the FWHM-width increased from 0.35 μm at 1 nJ (two times the threshold energy) to about 0.7 μm at 5 nJ [see Fig. 6(a)]. Compared to repetition rates below 4 MHz, the slope was significantly steeper at 80 MHz. At 100 pulses per micrometer, the increase of the FWHM-width between two and five times the threshold energy was about 20% stronger at 80 MHz than in the kHz regime [see Fig. 6(b)].

4. Discussion and conclusion

The presented results provide new insights into the mechanisms of femtosecond (fs) laser-based intracellular nanosurgery in the low-density plasma regime. As the localization of multiphoton

#132149 - $15.00 USD Received 22 Jul 2010; revised 5 Aug 2010; accepted 5 Aug 2010; published 10 Aug 2010

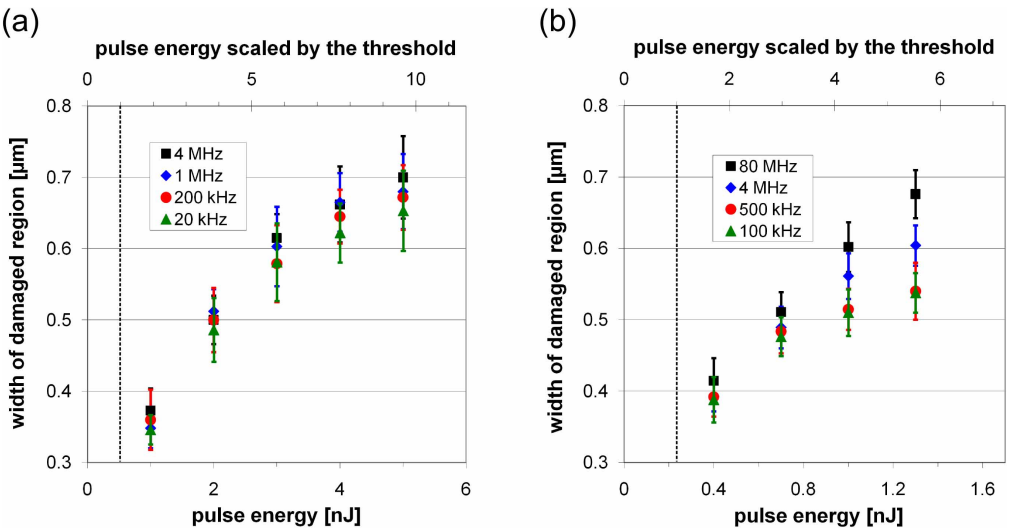

Fig. 6. FWHM-widths of the damaged region in live Hoechst stained cell nuclei as a function of the pulse energy at a central wavelength of 720 nm and different repetition rates. The dashed lines indicate the ablation threshold. Each data point represents the mean ± standard deviation of at least ten cells. (a) 2,000 pulses per micrometer and (b) 40,000 pulses per micrometer were used. No significant influence of the repetition rate was observed up to 4 MHz. The increase of the FWHM-width was significantly stronger at 80 MHz.

absorption is maintained even in strongly scattering tissue [28], the findings of this in-vitro study can also be applied to in-vivo experiments (e.g. [6-9]).

To the best of our knowledge, no systematic study of the influence of the laser wavelength and repetition rate on the intracellular ablation threshold has been done to date. In our experiments, we used Hoechst-stained cell nuclei as a model substance for intracellular nanosurgery, as fluorophores are usually required to enhance the weak contrast between subcellular structures [4, 11, 12].

At a constant radiant energy density (total laser energy per volume), the ablation threshold for line cuts in stained cell nuclei slightly decreased with increasing repetition rate from 1 kHz to 80 MHz. However, this difference was not significant [see Fig. 3(a)]. From this result, two conclusions can be drawn: thermal damage at high repetition rates does not play a significant role and the ablation effect results predominantly from the accumulation of single-shot photochemical damage. The first statement is supported by calculations of the temperature evolution in the focal volume in aqueous solution [10]. At the wavelength and numerical aperture used in our experiments, the temperature increase is expected to be below 3^{o}C at the ablation threshold, even at high repetition rates around 80 MHz. As thermal effects can be neglected, free-radical and free-electron induced chemical effects are most likely responsible for intracellular ablation (see introduction). Based on the results in Fig. 3(a), we can deduce that the photochemical processes of each pulse are finished within approximately 10 ns, being the time interval between two successive pulses at 80 MHz. If these processes originate from one-photon absorption, the exposure time would be inversely proportional to the irradiance as stated by the so-called reciprocity law in photobiology [29]. Our experiments revealed that the exposure time was inversely proportional to approximately the fourth power of irradiance at the ablation threshold [see Fig. 3(b)]. This indicates that multiphoton absorption is the precursor for chemical damage during intracellular nanosurgery.

#132149 - $15.00 USD Received 22 Jul 2010; revised 5 Aug 2010; accepted 5 Aug 2010; published 10 Aug 2010

Nikogosyan et al. showed that the hydroxyl radical ($OH^{\bullet}$) is the only free radical produced in sufficient amounts within a few nanoseconds [21]. The hydroxyl radical efficiently reacts with biomolecules, such as DNA, at diffusion-controlled rates [22]. Its half-life period in living cells is between 1 and 10 ns corresponding to the value estimated from our experiments [30, 31]. In a previous publication by our group, we showed that the total amount of free radicals was significantly decreased with an additional antioxidant in the culture medium [25]. However, no change of the ablation threshold pulse energy was observed at the same concentration (data not shown). As the hydroxyl radical is very reactive, high antioxidant concentrations in the molar range are required to observe a $OH^{\bullet}$-scavenging effect which do not correspond to physiological conditions [32]. Thus, only relatively unreactive radicals, which are not responsible for intracellular ablation, can be scavenged at the conditions used in our experiments.

Although the calculations of optical breakdown thresholds by Vogel et al. are in very good agreement with experimental results in aqueous solution [10, 18], the used model neglected the influence of dye and biomolecules on the multiphoton and cascade ionization rates. Therefore, the course of the free-electron density as a function of the laser pulse energy may significantly differ in a cellular environment. To study the influence of dye molecules, we compared the ablation probabilities both with and without Hoechst staining before line cutting. Without previous staining, about a factor four higher pulse energies were required for the same ablation probability [see Fig. 4(b)]. This behavior has also been observed by other authors investigating the ablation threshold in single chromosomes and the threshold for DNA double-strand break (DSB) formation. Koenig et al. observed a reduction of the ablation threshold by a factor of 2.7 when single chromosomes were labeled with Giemsa [2]. In addition, four [33] to ten times [34] more pulse energy was required to induce DSBs in cells without Hoechst staining. Consequently, dye molecules significantly contribute to the production of free electrons and hence the formation of low-density plasmas. According to the literature, a cell nucleus consists of 85% water [35], 20% of the nuclear dry mass is DNA [36] and one bound Hoechst molecule exists per ten base pairs at the used dye concentration [37]. Thus, the ratio of water to Hoechst molecules is approximately 10,000:1. From this calculation, we can conclude that Hoechst molecules do not significantly contribute to the cascade ionization. However, because of their high multiphoton absorption cross-section [38], they should enhance the multiphoton ionization rate to provide additional seed electrons for the following cascade.

In the low-density plasma regime, chemical effects accumulate with increasing number of laser pulses, leading to a lower ablation threshold pulse energy. This has been studied by several groups in dielectrics and metals as well as in biological tissue [16, 39, 40]. The dependence of the threshold pulse energy on the number of pulses can be described according to [40]:

$$E_N = E_1 \cdot N^{-1/k} \tag{1}$$

where N is the number of pulses and k describes the strength of the accumulation. E_1 and E_N are the threshold pulse energies for a single shot and N pulses, respectively. Our experiments revealed that the accumulation strength, being equivalent to the scaling exponent in Fig. 5, was dependent on the laser wavelength and repetition rate [see Fig. 5(b)]. In the kHz regime, the accumulation strength was constant for all wavelengths between 720 and 840 nm (k=4). By contrast, this value increased from k=3.5 to k=4 at 80 MHz repetition rate in the same wavelength range. Quite surprisingly, an increase of the accumulation strength from k=4 to k=5 occurred between 840 and 950 nm for all repetition rates.

As described earlier in the discussion, intracellular ablation most likely results from multiphoton-induced chemistry accumulating over multiple pulses. If we assume that laser pulses do not significantly change the optical properties of the focal volume up to the ablation effect, the damage to cellular structures should be the same for each pulse. Consequently, the

#132149 - $15.00 USD Received 22 Jul 2010; revised 5 Aug 2010; accepted 5 Aug 2010; published 10 Aug 2010

ablation effect for multiple pulses would be an accumulation of single-shot damage. This leads to the same equation as Eq. (1), in which the accumulation strength is equivalent to the multiphoton order inducing the photochemical effects. Following this model, four and five photons are required to induce damage to the DNA molecules at 840 and 950 nm, respectively, whereas both four- and five-photon induced processes occur at 900 nm (k=4.3). As multiphoton ionization yields the seed electrons for the ionization cascade and hence free-electron and free-radical induced chemical effects, we assume that the multiphoton order corresponds to the number of photons required for this process. Based on the results in Fig. 5(b), the ionization energy should be between 5.2 and 5.9 eV which excludes water having a band-gap of 6.5 eV [21, 41]. However, it corresponds well to that of Hoechst molecules (approx. 5.5 eV) [42]. Therefore, Hoechst molecules are most likely the major source for providing seed electrons.

To support this hypothesis, we did similar experiments with RAT-1 fibroblasts stably expressing the enhanced green fluorescent protein (eGFP) in the whole cell. Fitting of the ablation threshold data with Eq. (1) yielded an accumulation strength of k=3 between 720 and 820 nm. The same value has been obtained by Bourgeois et al. who used a wavelength of 780 nm at 1 kHz to ablate GFP-labeled motor neurons [16]. Above 860 nm, however, we observed an increase of the accumulation strength to k=4. Thus, the ionization energy of the major source for seed electrons should be between 4.3 and 4.5 eV corresponding to that of the single tryptophan residue of eGFP (approx. 4.5 eV) [43].

With the proposed model, the decrease of the accumulation strength at 80 MHz repetition rate and wavelengths below 840 nm can be explained [see Fig. 5(b)]. Free electrons become hydrated within 300 fs with a lifetime of around 0.25 μs in concentrated solutions of biomolecules [23]. Therefore, many of them are still present when the next laser pulse arrives at repetition rates above 4 MHz. As hydrated electrons absorb in the NIR wavelength range with a maximum at 720 nm [21], seed electrons are also produced by linear absorption at high repetition rates. The resulting accumulation strength is a mixture between multiphoton ionization of Hoechst molecules and linear absorption of hydrated electrons, leading to the observed values (e.g. k=3.5 at 720 nm). Because of the production of additional seed electrons at high repetition rates, the width of the damaged region increased significantly stronger compared to the kHz regime [see Fig. 6(b)].

In conclusion, we showed that the free-electron and free-radical induced chemical effects during fs laser-based intracellular nanosurgery are finished within a few nanoseconds. Thus, the ablation effect results from the accumulation of single-shot damage at kHz and MHz repetition rates. In addition, we demonstrated the strong influence of dye molecules on the ablation threshold. Future calculations of free-electron densities for intracellular nanosurgery have to take them into account, especially in the calculations of the multiphoton ionization rates. To minimize the total delivered laser energy to cells, it is advantageous to use high repetition rates at wavelengths between 700 and 800 nm, as residual hydrated electrons can easily be ionized by linear absorption in this regime.

Acknowledgments

We thank Alfred Vogel (Institute of Biomedical Optics, University of Luebeck, Germany) for stimulating discussions on the effects of low-density plasmas. This work is supported by funding from the Deutsche Forschungsgemeinschaft (DFG, German Research Foundation) within the Cluster of Excellence ”REBIRTH” (From Regenerative Biology to Reconstructive Therapy).

#132149 - $15.00 USD Received 22 Jul 2010; revised 5 Aug 2010; accepted 5 Aug 2010; published 10 Aug 2010